ACS APPLIED MATERIALS & INTERFACES

Research Article

www.acsami.org

Hybrid Composite $Ni(OH)_2$@$NiCo_2O_4$ Grown on Carbon Fiber Paper for High-Performance Supercapacitors

Liang Huang,[†,‡] Dongchang Chen,[‡] Yong Ding,[‡] Zhong Lin Wang,[‡] Zhengzhi Zeng,[†] and Meilin Liu*[,‡]

[†]Key Laboratory of Nonferrous Metal Chemistry and Resources Utilization of Gansu Province, College of Chemistry and Chemical Engineering, Lanzhou University, Lanzhou 730000, China

[‡]School of Materials Science and Engineering, Georgia Institute of Technology, 771 Ferst Drive, Atlanta, Georgia 30332-0245, United States

Supporting Information

ABSTRACT: We have successfully fabricated and tested the electrochemical performance of supercapacitor electrodes consisting of $Ni(OH)_2$ nanosheets coated on $NiCo_2O_4$ nanosheets grown on carbon fiber paper (CFP) current collectors. When the $NiCo_2O_4$ nanosheets are replaced by Co_3O_4 nanosheets, however, the energy and power density as well as the rate capability of the electrodes are significantly reduced, most likely due to the lower conductivity of Co_3O_4 than that of $NiCo_2O_4$. The 3D hybrid composite $Ni(OH)_2$/$NiCo_2O_4$/CFP electrodes demonstrate a high areal capacitance of 5.2 F/cm^2 at a cycling current density of 2 mA/cm^2, with a capacitance retention of 79% as the cycling current density was increased from 2 to 50 mA/cm^2. The remarkable performance of these hybrid composite electrodes implies that supercapacitors based on them have potential for many practical applications.

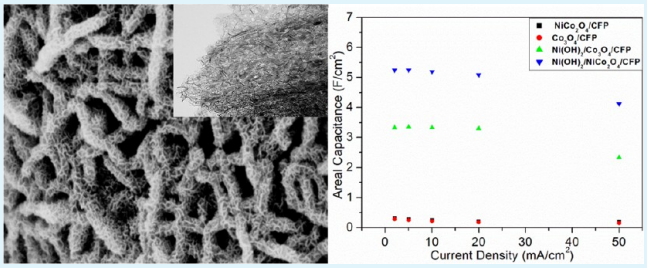

KEYWORDS: *energy storage, supercapacitor, carbon fiber, cobalt oxide, hybrid, composite*

Electrical energy storage and conversion systems play a vital role in efficient and cost-effective utilization of clean energy from renewable sources.[1−3] In particular, electrochemical energy storage and conversion devices such as batteries, fuel cells, and supercapacitors are considered the most promising candidate for portable and mobile applications.[4] Among them, supercapacitors offer a number of advantages over conventional batteries, including fast charge rate, long-term cycling stability, and the ability to deliver up to ten times more power. These features are desirable for a range of applications, from electric vehicles to smart grids.[5−10] Pseudocapacitors (with reversible Faradaic redox reactions at the electrode surfaces) usually offer much higher specific capacitance than supercapacitors made of carbonaceous materials based on double-layer charge storage.[11−14] Transition metal oxides and hydroxides are the most popular materials for the electrodes of pseudoapacitors because of their high theoretical capacitance, low cost, and low toxicity.[15−18] However, the experimentally obtainable values are often much lower than the theoretical expectations, especially when operated at high cycling rate, while the conductivity of the electrodes may be limited.

Recently three-dimensional (3D) hybrid electrodes have been used for pseudocapacitors. With large surface area and short diffusion path for electrons and ions, 3D hybrid structures are well-suited architectures for high-performance supercapacitor electrodes.[11,19−23]Here, we report a binder-free hybrid composite electrode with nanoarchitecture $Ni(OH)_2$/$NiCo_2O_4$ directly grown on carbon fiber paper (CFP). Comparing with a similar structure such as $NiCo_2O_4$ sheets and $Ni(OH)_2$/CoO walls on a metal substrate, our hybrid composite $Ni(OH)_2$/$NiCo_2O_4$/CFP could offer superior capacity and rate capability.[16,20]

The hybrid composite electrode was prepared by a facile two-step method. First, $NiCo_2O_4$ nanosheets were grown on CFP using an electrodeposition process followed annealing at 300 °C for 2 h.[16] Then, another layer of $Ni(OH)_2$ was grown on the $NiCo_2O_4$ sheets by a second electrodeposition process, as described in the Supporting Information. The uniform morphology of the $NiCo_2O_4$ nanosheets grown on CFP is shown in Figure 1a. The TEM image illustrates that the $NiCo_2O_4$ sheets are a porous structure composed of 10−20 nm nanocrystallites with pores 2−4 nm in diameter.(Figure 1b, Figure S1 in the Supporting Information) The HRTEM and SAED show the poly crystalline phase of these sheets with the thickness of several nanometers. (Figure 1c, d) After the second growth of $Ni(OH)_2$, the ultrathin sheets were converted to thick walls, as illustrated in Figure 1e. As can be seen from the Figure 1f, the $Ni(OH)_2$ layer on the surface of $NiCo_2O_4$ is also constructed by small ultrathin sheets. The X-ray diffraction pattern shows that the hybrid structure contains cubic $NiCo_2O_4$ with a space group of *Fd*3*m* (JCPDS Card No.73-1702) and *α*-$Ni(OH)_2$ phase (38−0715) (see Figure S4 in the Supporting Information). This 3D hybrid composite $Ni(OH)_2$/$NiCo_2O_4$ on

Received: August 15, 2013
Accepted: October 11, 2013
Published: October 11, 2013

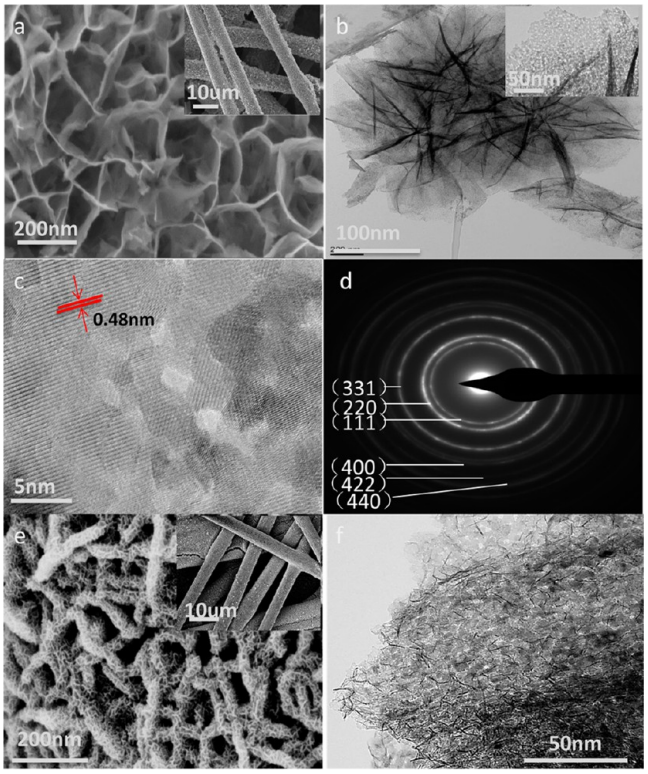

Figure 1. (a) SEM image of CFP after growth of $NiCo_2O_4$ nanosheets; (b, c) TEM image and HRTEM image of $NiCo_2O_4$ nanosheets. (d) Diffraction pattern of a $NiCo_2O_4$ nanosheets. (e) SEM image of a $Ni(OH)_2$ coating on $NiCo_2O_4$ nanosheets grown on CFP. (f) TEM image of $Ni(OH)_2/NiCo_2O_4$ hybrid composite grown on CFP.

the CFP with large surface area could offer favorable access to the electrolyte and enhance the ionic conductivity. The porous $NiCo_2O_4$ between CFP and $Ni(OH)_2$ could increase the electronic conduction through the electrode and allows high utilization of active materials. All these features of this hybrid electrode offer the potential for high-performance supercapacitors. To confirm the advantage of $NiCo_2O_4$ for high performance of this electrode, we prepared a $Ni(OH)_2/Co_3O_4$/CFP electrode (without adding the Ni source in the first step) for direct comparison under the same conditions (see Figures S2 and S3 in the Supporting Information)

Further, Raman spectroscopy was also used to characterize the phase composition of the $Ni(OH)_2/NiCo_2O_4$ hybrid structure. As seen in Figure S5 in the Supporting Information, the peaks at 186, 480, 529, and 668 cm^{-1} correspond to F_{2g}, E_g, F_{2g}, and A_{1g} models of the $NiCo_2O_4$ sheets, respectively[25] (see Figure S5 in the Supporting Information). After electrodeposition of a $Ni(OH)_2$ coating, a new peak at 527 cm^{-1} was observed, corresponding to the stretching Ni−O (H) bond.[11,24]

Then, we investigated the electrochemical performance of the hybrid composite $Ni(OH)_2/NiCo_2O_4$/CFP and $Ni(OH)_2/Co_3O_4$/CFP in the supercapacitors electrode application. All the measurement was carried out in a three-electrode cell system with 1 M KOH solution as electrolyte. The cyclic voltammetry (CV) performance of $NiCo_2O_4$/CFP and Co_3O_4/CFP before and after the deposition of $Ni(OH)_2$ at a scan rate of 5 mV/s in the potential window of 0−0.6 V is shown in Figure 2a. Without coating $Ni(OH)_2$, the Co_3O_4/CFP and $NiCo_2O_4$/CFP just show very weak redox peak, indicating poor electrochemical performance. After coating the $Ni(OH)_2$ for 10 min, a significant enhancement in the CV curve with a pair of redox peaks is observed, which can be attributed to the reversible Faradaic redox reactions of $Ni(OH)_2$ materials. The redox potential at 0.4−0.5 V for $Ni(OH)_2/NiCo_2O_4$/CFP and $Ni(OH)_2/Co_3O_4$/CFP also matches the previous report used $Ni(OH)_2$ as active materials for the supercapacitors application.[25] Analysis of the CV curves suggest that both Co_3O_4/CFP and $NiCo_2O_4$/CFP may serve mainly as the current collector, making little contribution to the capacitance of the electrodes.

The galvanostatic charge−discharge characteristic of hybrid composite within the potential range of 0−0.45 V at a current density of 5 mA/cm^2 is shown in Figure2b. Obviously, the discharge curve can be divided into two sections, a sudden potential drop due to the internal resistance and a slow potential decay due to the Faradic redox reaction. This phenomenon suggests the pseudo-capacitance in our cell system (see Figure S6 in the Supporting Information). The areal capacitance (AC) and specific capacitance (SC) were calculated using eqs 1 and 2 (Supporting information). The AC of the $Ni(OH)_2/NiCo_2O_4$/CFP and $Ni(OH)_2/Co_3O_4$/CFP at a current density of 5 mA/cm^2 is 5.2 and 3.3 F/cm^2, respectively, which is ∼18 and ∼12 times higher than the AC of $NiCo_2O_4$/CFP and Co_3O_4/CFP at the same current density. (Figure 2c) The highest SC of $Ni(OH)_2/NiCo_2O_4$/CFP and $Ni(OH)_2/Co_3O_4$/CFP base on the total mass (including the weight of CFP, metal oxide and hydroxyl oxide) is 464 and 291 F/g, respectively, with capacitance retention of 78 and 69% as the current density is increased from 2 to 50 mA/cm^2. This performance is superior to that previously reported for the $Ni(OH)_2$/CoO walls on the nickel foam, which showed a capacitance retention of 57% when the current density was increased from 2 to 40 mA/cm^2.[20] (Figure 2d) The remarkable performance and rate capability of $Ni(OH)_2/NiCo_2O_4$/CFP, compared to $Ni(OH)_2/Co_3O_4$/CFP, the higher conductivity of $NiCo_2O_4$ than Co_3O_4, which improve the utilization of $Ni(OH)_2$ coating during cycling. In fact, when the mass of CFP is excluded (i.e., only the mass of metal oxide and hydroxide is considered) in the calculation of capacitance per unit weight of active materials, the specific capacitance of hybrid composite $Ni(OH)_2/NiCo_2O_4$ is ∼3200 F/g at a current density of 2 mA/cm^2 (see Figure S7 in the Supporting Information).

The cycle life of these hybrid composite electrodes over 1 000 cycles was tested at a current density of 5 mA/cm^2 under galvanostatic charge/discharge cycling in the potential range from 0 to 0.45 V. As shown in Figure S8 in the Supporting Information, the areal capacitance of $Ni(OH)_2/Co_3O_4$/CFP and $Ni(OH)_2/NiCo_2O_4$/CFP dropped over 64% after 1 000 cycles, but impressive areal and specific capacitances as well as the rate capability suggest that the hybrid structure are suited for high-performance supercapacitors. Moreover, the morphology of $Ni(OH)_2/NiCo_2O_4$/CFP was retained well after 1000 cycles, indicating a highly stabile architecture of this hybrid composite. (Figure 3) To identify the cause of the performance loss during cycling, we performed thermogravimetric analysis (TGA) and BET surface area analysis of hybrid composite samples before and after the cycling measurements. The TGA data suggest that the mass of the active materials ($Ni(OH)_2/NiCo_2O_4$) is relatively stable during the cycling (the mass loading still remained at ∼16%). However, the specific surface area of the hybrid composite electrodes decreased more than 80% after 1000 cycles, as shown in Figure S10 in the Supporting Information. Thus, the decrease in specific surface area is the main cause of the poor cycling stability of the $Ni(OH)_2/NiCo_2O_4$/CFP.

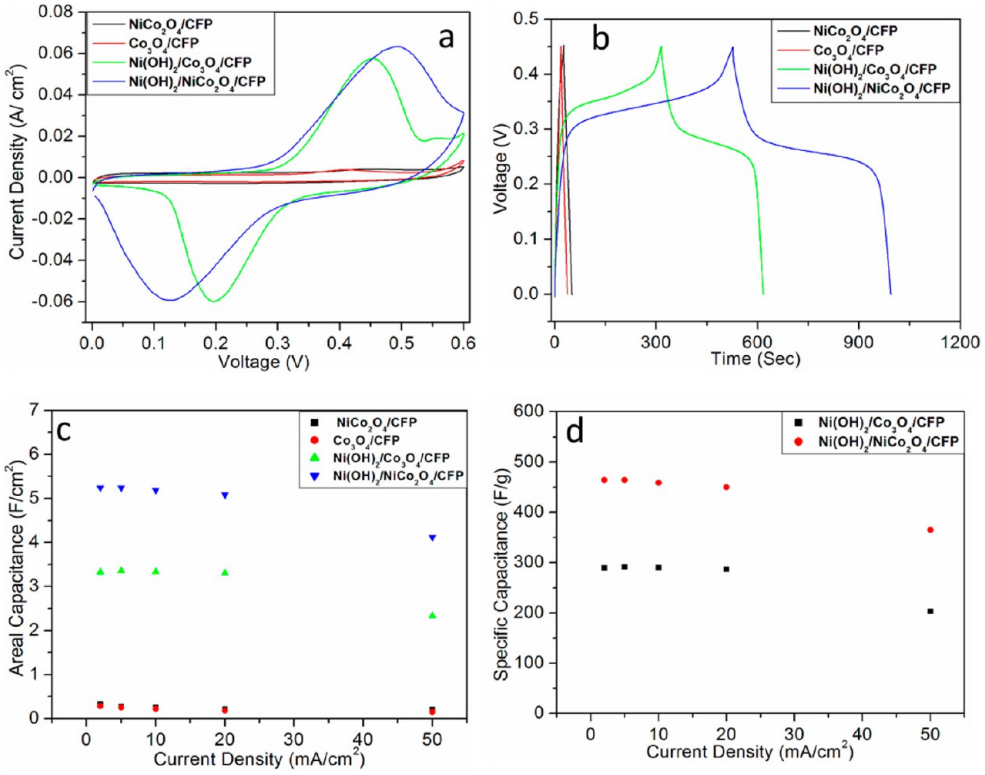

Figure 2. (a) Cyclic voltammograms of $NiCo_2O_4$/CFP, Co_3O_4/CFP, $Ni(OH)_2/Co_3O_4$/CFP, and $Ni(OH)_2/NiCo_2O_4$/CFP composite electrode in a 3-electrode cell with 1M KOH aqueous solution at scan rates of 5 mV/s. (b) Charge and discharge curves of hybrid composite electrodes at a current density of 5 mA/cm^2. (c) Areal capacitances of hybrid composite electrodes at different current densities. (d) Specific capacitance of hybrid composite electrodes at different current density (base on total mass of electrode).

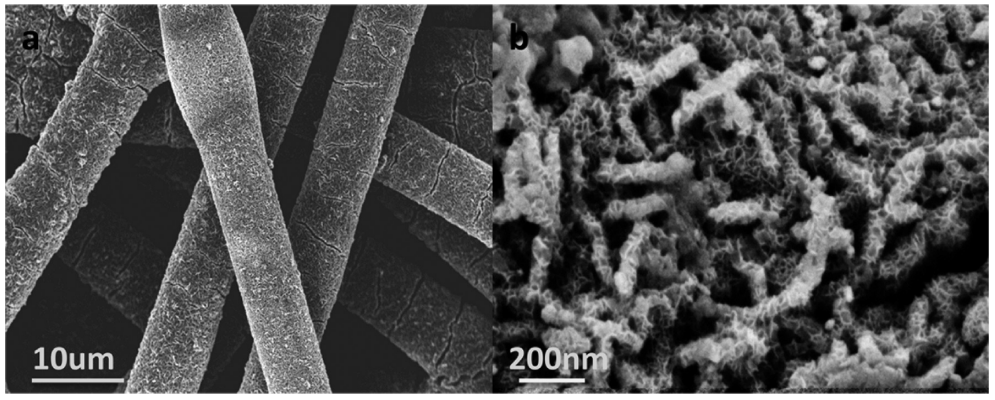

Figure 3. (a, b) Low- and high-magnification SEM image of $Ni(OH)_2/NiCo_2O_4$/CFP after 1000 cycles at current density of 5 mA/cm^2.

Careful analyses of the microstructures of the $Ni(OH)_2/NiCo_2O_4$/CFP electrodes suggest that their high specific capacitance and remarkable rate capability when used as electrochemical pseudocapacitors, are attributed to the following unique features. First, the CFP network with high conductivity allows efficient current collection or rapid electron transport to and from the electrochemically active materials. Second, the mesoporous, ultrathin $NiCo_2O_4$ sheets and $Ni(OH)_2$ plates provide sufficient open spaces and a shorter ion diffusion path for fast ionic transport, leading to higher utilization of active materials.

In summary, hybrid composites $Ni(OH)_2/Co_3O_4$ and $Ni(OH)_2/NiCo_2O_4$ directly grown on CFP were used as electrodes for supercapacitors. The electrochemical performances of the $Ni(OH)_2/NiCo_2O_4$/CFP are better than those of the $Ni(OH)_2/Co_3O_4$/CFP electrode, demonstrating higher specific capacitance and rate capability. The capacitance retention is about 79% as the cycling current density was increased from 2 to 50 mA/cm^2.

■ ASSOCIATED CONTENT

Ⓢ Supporting Information

Synthesis detail of hybrid composite $Ni(OH)_2/NiCo_2O_4$ and $Ni(OH)_2/Co_3O_4$. This material is available free of charge via the Internet at http://pubs.acs.org.

■ AUTHOR INFORMATION

Corresponding Author

*E-mail: meilin.liu@mse.gatech.edu. Phone:404-894-6114.

Notes

The authors declare no competing financial interest.

■ ACKNOWLEDGMENTS

This material is based upon work supported as part of a DOE ARPA-E project under Award Number DE-AR0000303. Liang Huang thanks for a fellowship from the China Scholarship Council.

■ REFERENCES

(1) Wang, G.P.; Zhang, L.; Zhang, J.J. *Chem. Soc. Rev.* **2012**, *41*, 797−828.
(2) Tian, B.; Zheng, X.; Kempa, T. J.; Fang, Y.; Yu, N.; Yu, G.; Huang, J.; Lieber, C. M. *Nature.* **2007**, *449*, 885.
(3) Wang, X. D.; Song, J. H.; Liu, J.; Wang, Z. L. *Science.* **2007**, *316*, 102.
(4) Winter, M.; Brodd, R. J. *Chem. Rev.* **2004**, *104*, 4245−4269.
(5) Stoller, M.D.; Ruoff, R.S. *Energy Environ. Sci.* **2010**, *3*, 1294−1301.
(6) Choi, D.; Kumta, P. N. *Electrochem. Solid-State Lett.* **2005**, *8*, A418−A422.
(7) Wei, W. F.; Cui, X.; Chen, W.; Ivey, D. G. *Chem. Soc. Rev.* **2011**, *40*, 1697−1721.
(8) Simon, P.; Gogotsi, Y. *Nat. Mater.* **2008**, *7*, 845−854.
(9) Zheng, J. P. *Electrochem. Solid-State Lett.* **1999**, *2*, 359−361.
(10) Yu, G. H.; Xie, X.; Bao, Z. N.; Cui, Y. *Nano Energy.* **2013**, *2*, 213−234.
(11) Huang, L.; Chen, D. C.; Ding, Y.; Feng, S.; Wang, Z. L.; Liu, M. L. *Nano Lett.* **2013**, *13*, 3135−3139.
(12) Yang, L.; Cheng, S.; Ding, Y.; Zhu, X. B.; Wang, Z. L.; Liu, M. L. *Nano Lett.* **2012**, *12*, 321−325.
(13) Zhou, W. J.; Cao, X.; Zeng, Z. Y.; Shi, W. H.; Zhu, Y. Y.; Yan, Q. Y.; Liu, H.; Zhang, H. *Energy Environ. Sci.* **2013**, *6*, 2216−2221.
(14) Wang, H. L.; Casalongue, H. S.; Liang, Y.Y.; Dai, H. J. *J. Am. Chem. Soc.* **2010**, *132*, 7472−7477.
(15) Xu, J.; Wang, Q. F.; Wang, X. W.; Xiang, Q. Y.; Liang, B.; Chen, Di.; Shen, G. Z. *ACS Nano* **2013**, *7*, 5453−5462.
(16) Yuan, C. Z.; Li, J.Y.; Hou, L.R.; Zhang, X. G.; Shen, L.F.; Lou, X. W. *Adv. Funct. Mater.* **2012**, *22*, 4592−4597.
(17) Shang, C.Q.; Dong, S.; Wang, S.; Xiao, D. D.; Han, P. X.; Wang, X. G.; Lin, G.; Cui, G. L. *ACS Nano* **2013**, *7*, 5430−5436.
(18) Zhou, C.; Zhang, Y. W.; Li, Y. Y.; Liu, J. P. *Nano Lett.* **2013**, *13*, 2078−2085.
(19) Tian, W.; Wang, X.; Zhi, C.Y.; Zhai, T. Y.; Liu, D. Q.; Zhang, C.; Golberg, D.; Bando, Y. *Nano Energy*. http://dx.doi.org/10.1016/j.nanoen.2013.01.004
(20) Guan, C.; Li, X. L.; Wang, Z. L.; Cao, X. H.; Soci, C.; Zhang, H.; Fan, H. J. *Adv. Mater.* **2012**, *24*, 4186−4190.
(21) Tang, Z.; Tang, C. H.; Gong, H. *Adv. Funct. Mater.* **2012**, *22*, 1272−1278.
(22) Liu, J. P.; Jiang, J.; Cheng, C. W.; Li, H. G.; Zhang, J. X.; Fan, H. J. *Adv. Mater.* **2011**, *23*, 2076−2081.
(23) Guan, C.; Liu, J. P.; Cheng, C.W.; Li, H. X.; Li, X. L.; Zhou, W. W.; Zhang, H.; Fan, H. J. *Energy Environ. Sci.* **2011**, *4*, 4496−4499.
(24) Vidotti, M.; Salvador, R.P.; Torresi, S. I. C *Ultrasonics Sonochem* **2009**, *16*, 35.
(25) Yang, G. W.; Xu, C. L.; Li, H.L. *Chem. Commun.* **2008**, 6537−6539. <!——>